A Novel RNA-Binding Protein Associated with Cell Plate Formation[1][C][W][OA]

Lian Ma, Bo Xie, Zonglie Hong, Desh Pal S. Verma, and Zhongming Zhang*

State Key Laboratory of Agricultural Microbiology, Huazhong Agricultural University, Wuhan 430070, China (L.M., Z.Z.); College of Life Science, Yangtze University, Jingzhou 434025, China (L.M.); Department of Microbiology, Molecular Biology, and Biochemistry, University of Idaho, Moscow, Idaho 83844–3052 (B.X., Z.H.); and Department of Molecular Genetics and Plant Biotechnology Center, Ohio State University, Columbus, Ohio 43210–1002 (D.P.S.V.)

Building a cell plate during cytokinesis in plant cells requires the participation of a number of proteins in a multistep process. We previously identified phragmoplastin as a cell plate-specific protein involved in creating a tubulovesicular network at the cell plate. We report here the identification and characterization of a phragmoplastin-interacting protein, PHIP1, in Arabidopsis (*Arabidopsis thaliana*). It contains multiple functional motifs, including a lysine-rich domain, two RNA recognition motifs, and three CCHC-type zinc fingers. Polypeptides with similar motif structures were found only in plant protein databases, but not in the sequenced prokaryotic, fungal, and animal genomes, suggesting that PHIP1 represents a plant-specific RNA-binding protein. In addition to phragmoplastin, two Arabidopsis small GTP-binding proteins, Rop1 and Ran2, are also found to interact with PHIP1. The zinc fingers of PHIP1 were not required for its interaction with Rop1 and phragmoplastin, but they may participate in its binding with the *Ran2* mRNA. Immunofluorescence, in situ RNA hybridization, and green fluorescent protein tagging experiments showed the association of PHIP1 with the forming cell plate during cytokinesis. Taken together, our data suggest that PHIP1 is a novel RNA-binding protein and may play a unique role in the polarized mRNA transport to the vicinity of the cell plate.

Cytokinesis in higher plants is marked by the formation of phragmoplast that is initiated in late anaphase and continues through telophase of the cell cycle. The cell plate, a disc-like structure, is formed in the center of the phragmoplast and expands in a plane between the two daughter nuclei until it reaches the parental cell wall (Samuels et al., 1995; Staehelin and Hepler, 1996; Verma, 2001). Although the phragmoplast structure was known for a long time, no specific protein marker for this ''organelle'' was available until phragmoplastin was identified (Gu and Verma, 1996).

Building the cell plate from Golgi-derived vesicles is a multistep process. Golgi-derived vesicles are transported to the growing cell plate by sliding along the microtubules from the minus end to the plus end. The transport of vesicles may be driven by microtubule-associated motors such as kinesin-related proteins (Hong and Verma, 2008). Several stages of cell plate formation can be distinguished at the electron microscope level: delivery of vesicles from the Golgi apparatus to the equatorial plane, formation of a tubulovesicular network, consolidation of the tubular network and deposition of callose, fusion of the cell plate with the parental wall, and cellulose synthesis (Samuels et al., 1995; Staehelin and Hepler, 1996; Verma, 2001; Seguí-Simarro et al., 2004).

Phragmoplastin is a 68-kD GTPase related to the dynamin family of proteins, but it does not contain either the pleckstrin homology domain or the Pro-rich domain, both of which are characteristic of animal dynamins (Verma and Hong, 2005). It is present largely in the membrane fractions (presumably the Golgi-derived vesicles) and can also be detected in the cytosol (Gu and Verma, 1996). It contains two separable self-assembly domains (SA1 and SA2) that are responsible for the formation of phragmoplastin polymers (Zhang et al., 2000). Intermolecular interaction between SA1 and SA2 leads to the formation of staggered helical polymer structures that wrap around vesicles. Polymerization of phragmoplastin is dependent on GTP binding (Zhang et al., 2000) and may be regulated by other protein components (Verma, 2001; Verma and Hong, 2005). It has five closely related paralogs (DRP1A–DRP1E) in Arabidopsis (*Arabidopsis thaliana*;

[1] This work was supported by grants from the National Natural Science Foundation of China to Z.Z. (grant nos. 30070370 and 30570056), from the National Basic Research Program of China to Z.Z. (grant no. 01CB108901), and from the National Science Foundation to Z.H. (grant nos. NSF–MCB 0548525 and NSF–IOB 0543923) and to D.P.S.V. (grant nos. IBN–0095112 and NSF–IOS 0726284).

* Corresponding author; e-mail zmzhang@mail.hzau.edu.cn.

The authors responsible for distribution of materials integral to the findings presented in this article in accordance with the policy described in the Instructions for Authors (www.plantphysiol.org) are: Zhongming Zhang (zmzhang@mail.hzau.edu.cn) and Desh Pal S. Verma (verma.1@osu.edu).

[C] Some figures in this article are displayed in color online but in black and white in the print edition.

[W] The online version of this article contains Web-only data.

[OA] Open Access articles can be viewed online without a subscription.

www.plantphysiol.org/cgi/doi/10.1104/pp.108.120527

Hong et al., 2003), which appear to act as tubulases in creating dumbbell-shaped tubular structures at the cell plate (Verma, 2001; Verma and Hong, 2005).

Polarized intracellular RNA localization plays an essential role in cell fate determination during embryonic development, polar cell growth, cell motility, and seed development (Okita and Choi, 2002; Van de Bor and Davis, 2004; Crofts et al., 2005). It is an efficient way to target gene products to the proper subcellular locations. More than 100 different mRNAs, including those encoding rice (*Oryza sativa*) storage proteins and *Fucus actin* mRNA, have been documented to be targeted to specific locations before they are translated into peptides (Crofts et al., 2005). These mRNAs are targeted to discrete regions of the cell by different mechanisms, of which the RNA localization pathway is the predominant one (Okita and Choi, 2002). This pathway involves the formation of a ribonucleoprotein (RNP) complex and its movement along microtubule and microfilament tracks.

In this study, we identified an Arabidopsis protein as the phragmoplastin-interacting protein (PHIP1). Its deduced peptide contains several unique features, including a Lys (K)-rich domain (KRD), two RNA recognition motifs (RRMs), and three CCHC-type zinc fingers (ZnFs). It interacts with the Arabidopsis Rho-like GTPase, Rop1, in its GTP-bound configuration. It also binds specifically to the mRNA of another small GTPase, Ran2. PHIP1 colocalized with phragmoplastin at the cell plate and may play an essential role in targeting *Ran2* mRNA and possibly other cell plate formation-related mRNAs to the vicinity of the cell plate at cytokinesis in plants. Such a mechanism may allow the plant cell to rapidly build this subcellular compartment, completion of which is essential for proper cytokinesis.

RESULTS

Identification of Phragmoplastin-Interacting Proteins

Phragmoplastin is structurally and functionally conserved in different plants. Our previous studies indicated that phragmoplastin forms a complex not only with itself (self-assembly; Zhang et al., 2000) but also with other proteins at the cell plate (Gu and Verma, 1997; Hong et al., 2001a, 2001b). In an attempt to identify phragmoplastin-associated proteins, we screened an Arabidopsis cDNA library constructed in the yeast two-hybrid system (Kim et al., 1997). Approximately two million yeast colonies containing the phragmoplastin bait and the cDNA library preys were screened with the X-Gal blue/white staining test. One cDNA isolated from two independent yeast colonies was found to encode a protein (see below) designated PHIP1 (Fig. 1; Supplemental Fig. S1).

To assess which region of phragmoplastin interacts with PHIP1, we divided the phragmoplastin cDNA into two parts (Supplemental Fig. S1A). A *Bgl*II fragment encoding the N-terminal one-third of the molecule including the GTPase region was unable to interact with PHIP11. The *Hin*cII-*Bam*HI fragment encoding most of the dynamin homology II domain and part of the GTPase effector domain of phragmoplastin retained the ability to interact with PHIP1, suggesting that the interaction takes place through the C-terminal two-thirds of the phragmoplastin molecule. This interaction was further confirmed using an in vitro protein-protein interaction assay (Supplemental Fig. S2, lane 4; see below).

PHIP1 Is a Plant-Specific Protein

DNA sequencing of the PHIP1 insert revealed that it contained an open reading frame fused in-frame with the activating domain in the vector. Because the cDNA insert did not contain a start codon (ATG) and a stop codon, it apparently was not a full-length clone (PHIP-KRZ in Fig. 1). Using this insert as a probe, we screened two independent cDNA libraries and were able to obtain clones longer than the original insert at both the C and N termini. The clone obtained from the Arabidopsis cDNA library, CD4-15 (Arabidopsis Biological Resource Center, Ohio State University; Kieber et al., 1993), extended the insert 440 bp at the C terminus, including an in-frame stop codon and a

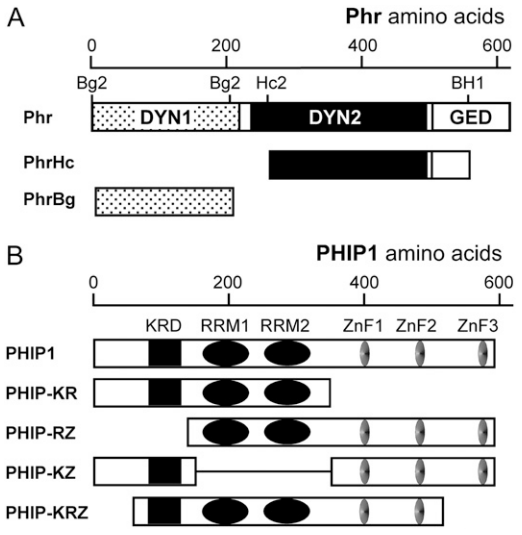

Figure 1. Functional domains and deletion constructs of phragmoplastin and PHIP1. A, Phragmoplastin contains three functional domains: the dynamin homology 1 (DYN1), DYN2, and a GTPase effector domain (GED). The PhrHc fragment containing DYN2 and part of GED is sufficient for interaction with PHIP1. Relative positions of restriction enzyme sites on the phragmoplastin cDNA are indicated: Bg2, *Bgl*II; Hc2, *Hin*cII; BH1, *Bam*HI. B, PHIP1 contains one KRD, two RRMs, and three CCHC-type ZnFs. Constructs containing different motifs were assayed for interaction with phragmoplastin and Rop1. PHIP-KRZ lacking the N terminus and the third ZnF was isolated from the library screen using phragmoplastin as bait. Deletion fragments containing KRD and RRM retained the ability to interact with both phragmoplastin and Rop1. Phr, Full-length phragmoplastin; PhrHc, the *Hin*cII-*Bam*HI fragment of phragmoplastin; PhrBg, the *Bgl*II fragment of phragmoplastin. ZnF1, ZnF2, and ZnF3 indicate the three ZnFs present in the C terminus of PHIP1.

stretch of nine poly(A). Screening of another cDNA library, FL-1 (Seki et al., 1998), resulted in an apparently full-length clone that extended 190 bp at the 5′ end. The full-length clone contains at position 27 an ATG codon within a sequence context matching the consensus for translation initiation in plant mRNAs (AACCATGGC; Lutcke et al., 1987), suggesting that this may be the translation initiation codon of the PHIP1 mRNA.

The full-length cDNA is 2,115 bp long and encodes a peptide of 597 amino acid residues with a calculated molecular mass of 65.8 kD (Supplemental Fig. S2A). It contains multiple functional motifs, including a KRD at the N terminus, two RRMs in the center of the molecule, and three CCHC-type ZnF domains at the C terminus (Supplemental Fig. S2B; see below). A database search using the deduced peptide sequence failed to identify homolog proteins with a similar arrangement of these functional motifs from prokaryotes, fungi, or animals, suggesting that it represents a plant-specific protein. *PHIP1* (At3g55340) is a unique gene in the Arabidopsis genome and has an ortholog gene in each of the two rice subspecies examined, Os05g0114500 in subspecies *japonica* and OsI_017529 in subspecies *indica*. The function of the rice orthologs has not been determined. The overall homology between the Arabidopsis PHIP1 and its rice orthologs is not very high (31% identity at the peptide level). However, they all contain the same functional motifs arranged in a similar manner, except that the rice proteins contain four CCHC-type ZnF domains as opposed to the three ZnFs present in PHIP1. Conservation of PHIP1 as a novel protein in higher plants is consistent with the unique nature of cytokinesis in plants (i.e. building of the cell plate de novo in the center of the phragmoplast).

PHIP1 Contains a KRD, Two RRMs, and Three ZnF Domains

Twenty Lys residues are clustered near the N terminus of PHIP1 between amino acid positions 83 and 131 (Supplemental Fig. S2, A–C). We term this domain the KRD. Three nuclear localization motifs (KKKR/NK) are found inside this sequence (Supplemental Fig. 2C). In addition to serving as nuclear localization signals, KRDs have also been implicated in nucleotide binding (Erard et al., 1998), protein-protein interactions (Huang and Kleinberg, 1999), and membrane association (Schwieger and Blume, 2007). The role of the KRD in PHIP1 remains unclear, although it is required for the interaction with phragmoplastin and Rop1 (see below).

Two copies of a truncated RRM are present in the middle of the PHIP1 molecule. RRM has been found in a number of RNA-binding proteins (Maris et al., 2005). It consists of two RNA-binding protein motifs, RNP-1 and RNP-2, separated by 30 amino acids (Dreyfuss et al., 1988). RNP-1 is an octapeptide with a consensus pattern of [RK]-G-{EDRKHPCG}-[AGSCI]-[FY]-[LIVA]-X-[FYLM], whereas RNP-2 is a hydrophobic segment of six residues. The full-length RRM spans approximately 90 amino acid residues. In PHIP1, both RRMs are slightly shorter, having only 78 amino acids (12 residues less than the consensus sequence). Both RRMs contain the two conserved core elements, RNP-1 and RNP-2 (Supplemental Fig. S2D).

Three copies of a CCHC-type ZnF (**C**YE**C**GEKG**H**L-ST/SA**C**) with a consensus of $CX_2CX_4HX_4C$ are present near the C terminus of PHIP1. They belong to the classical ZnFs that constitute a short β-hairpin and an α-helix with a zinc atom coordinated in a Cys-Cys-His-Cys manner (Gamsjaeger et al., 2007). This type of ZnF is often found in the nucleocapsid proteins of retroviruses and can facilitate intermolecular interactions between nucleic acids and proteins (Berg, 1986; Matthews and Sunde, 2002; Gamsjaeger et al., 2007). Unlike viral gag proteins that also contain CCHC-type ZnFs but are small molecules (fewer than 100 amino acid residues), PHIP1 is a relatively large molecule (about 600 amino acids) and has multiple functional motifs. Proteins with a similar type of CCHC, $CX_2CX_{12}HX_{3\text{-}5}C$, have also been implicated in protein-protein interactions (Tsang et al., 1997; Mackay and Crossley, 1998). The homology among the three copies of ZnFs extends to the sequences surrounding the ZnF motif, indicating that they might have evolved from intragenic duplications.

The Interaction between PHIP1 and Phragmoplastin Is Independent of ZnFs

Cognizant of the fact that CCHC ZnFs have been implicated in protein-protein interactions (Tsang et al., 1997; Mackay and Crossley, 1998; Gamsjaeger et al., 2007), we examined if the three copies of CCHC ZnFs are involved in the interaction between PHIP1 and phragmoplastin. A series of deletions of PHIP1 were constructed and tested for interaction with phragmoplastin in the yeast two-hybrid system. In comparison with the full-length PHIP1, deletion of the last ZnF (PHIP-Z2), the last two ZnFs (PHIP-Z1), or all three ZnFs (PHIP-KR) did not affect its interaction with phragmoplastin (Supplemental Fig. S3). These results demonstrated that the CCHC ZnFs are not involved in the interaction between PHIP1 and phragmoplastin. This conclusion was also supported by the result that the C-terminal half of PHIP1, containing all three ZnFs (PHIP-Z), was not able to interact with phragmoplastin (Supplemental Fig. S3). This interaction was apparently mediated via the N-terminal half of PHIP1, where KRD and RRM motifs are present. In an attempt to further determine if KRD or RRM is responsible for the interaction, we constructed three deletions (PHIP-RZ, PHIP-KZ, and PHIP-R) that contained, respectively, RRM plus ZnFs, KRD plus ZnFs, or RRM alone. All three deletions were unable to interact with phragmoplastin (Supplemental Fig. S3), suggesting that the structural integrity of the PHIP1 N terminus containing both KRD and RRMs is required for interaction with phragmoplastin.

PHIP1 Interacts with Rop1 in the GTP-Bound Configuration

The Arabidopsis Rho-like protein Rop1, when expressed in BY-2 cells, was found to be associated with the plasma membrane as well as with the forming cell plate at cytokinesis (Z. Hong, D.P.S. Verma, and Z. Zhang, unpublished data). We attempted but were unable to detect a direct interaction between Rop1 and phragmoplastin in the yeast two-hybrid system (data not shown). We then tested the possibility of an interaction between Rop1 and PHIP1. We expressed PHIP1 in yeast Y190 cells containing dominant positive (GTP-bound; Rop-GTP), wild-type (Rop-WT), or dominant negative (GDP-bound; Rop-GDP) forms of Rop1 expressed from the pAS2 vector (Wu et al., 2000). Protein-protein interactions were assayed in yeast colonies using X-Gal staining. Compared with the interaction between phragmoplastin and PHIP1, the interaction between Rop1 and PHIP1 was weaker (Fig. 2A). It required up to 12 to 24 h to develop blue color, while the interaction between phragmoplastin and PHIP1 took only 3 to 4 h. It is interesting that PHIP1 interacted only with the GTP-bound form of Rop1 but not the GDP-bound form. This may suggest a functional significance of this interaction.

To verify the interaction observed in the yeast two-hybrid system, we carried out an in vitro pull-down assay. Rop1 and phragmoplastin were purified as glutathione *S*-transferase (GST)-tagged proteins (Fig. 2B, lanes 2 and 3). GST served as a negative control (Fig. 2B, lane 1). PHIP-KRZ, the nearly full-length PHIP1 that was isolated from the original library screen (Fig. 1), was synthesized in vitro in the presence of [^{35}S]Met using the TNT T7 quick-coupled transcription/translation system (Promega; Fig. 2B, lane 4). ^{35}S-labeled PHIP1 was incubated with purified recombinant Rop1 or phragmoplastin bound to glutathione-agarose beads. As shown in Figure 2B, Rop1 and phragmoplastin were able to pull down a significant portion of ^{35}S-labeled PHIP1, whereas GST alone (negative control) did not retain any radiolabeled product. We also verified the interaction between Rop1 and deletion fragments of PHIP1 in a protein-protein pull-down assay. Our data demonstrated that both KRD and RRM motifs are required for the interaction and that the ZnFs are dispensable (Supplemental Fig. S4). These results further confirmed the specificities of interactions demonstrated by the yeast two-hybrid system. The data on in vitro interactions also suggest that no additional protein component is required for these interactions. Thus, PHIP1 appears to act as a sandwich between phragmoplastin and Rop1.

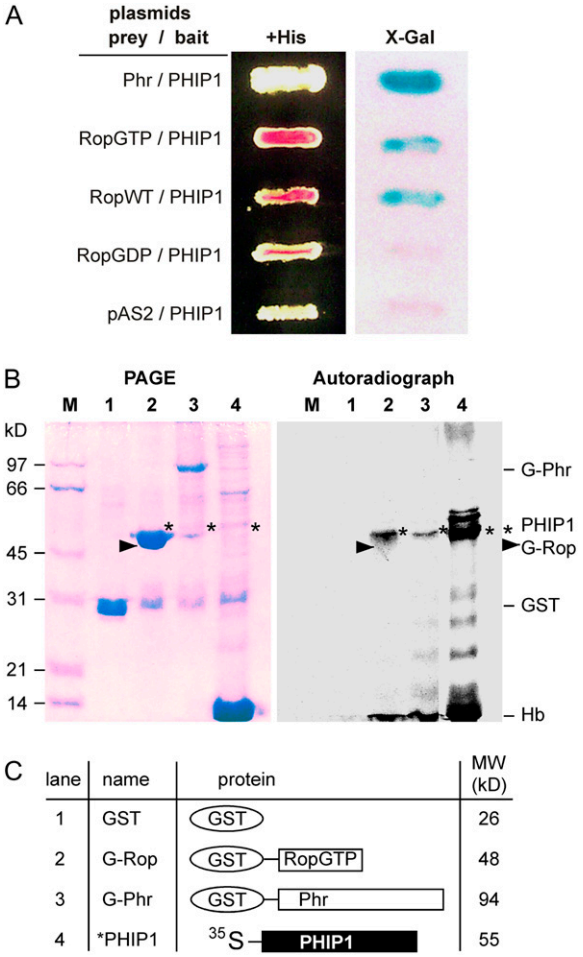

Figure 2. PHIP1 interacts with Rop1 in the yeast two-hybrid system and in vitro. A, Rop1 (RopWT), its dominant positive mutant (RopGTP), or its dominant negative mutant (RopGDP) was expressed in yeast cells using the pAS2 bait vector (see "Materials and Methods"). Plasmids were transformed to Y190 cells harboring pACT-PHIP1. Transformants were streaked on a propagation medium (+His), and the replica was stained for X-Gal activity (X-Gal). Plasmids pAS-Phr and pAS2 (vector alone) were used as positive and negative controls, respectively. B, Rop1 and phragmoplastin were purified through a GST tag (lanes 2 and 3). GST alone served as a negative control (lane 1). PHIP-KRZ, the nearly full-length PHIP1 that was isolated from the original library screen, was synthesized and labeled with [^{35}S]Met using the in vitro transcription/translation system (lane 4). [^{35}S]PHIP1 was incubated with either Rop1 or phragmoplastin bound to agarose beads. Proteins that were retained on the beads were eluted and resolved by SDS-PAGE. The gel stained with Coomassie Brilliant Blue R-250 was photographed (PAGE) and autoradiographed (Autoradiograph). Hb, Hemoglobin that is a by-product of the in vitro labeling system; M, molecular mass standards in kilodaltons. Asterisks indicate the bands of the pull-down ^{35}S-labeled PHIP1 (*PHIP1) on the autoradiograph and their relative positions on the PAGE gel. Arrowheads indicate the position of G-Rop1. C, Schematic representation of the protein components shown in B and their calculated molecular mass in kilodaltons. [See online article for color version of this figure.]

PHIP1 Is a Peripheral Membrane Protein

A hydrophilicity plot (Supplemental Fig. S2F) and membrane-spanning topology analyses revealed that PHIP1 is a highly hydrophilic protein with no transmembrane domain. The hydrophilic property is especially prominent at the N-terminal KRD region that is rich in Lys residues that carry positive charges under physiological conditions. The N terminus of PHIP1

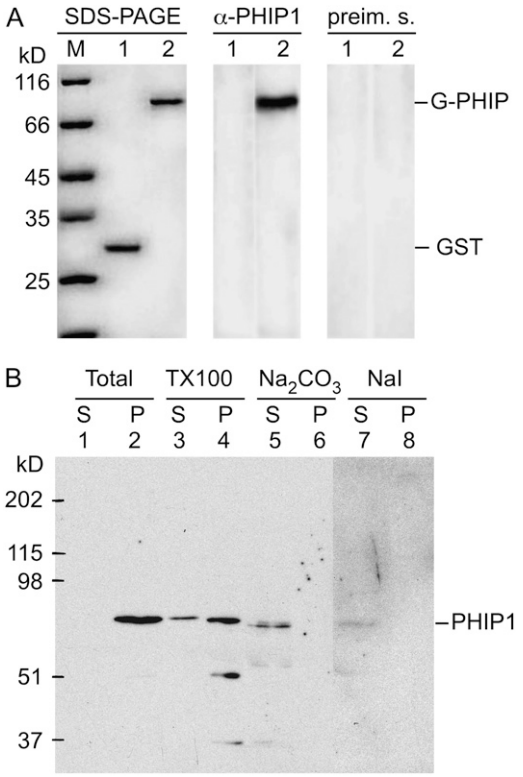

Figure 3. Western-blot analysis of PHIP1 in Arabidopsis plants. A, Specificity of polyclonal antibodies to PHIP1. Five micrograms of purified GST (negative control; lane 1) and GST-PHIP1 (lane 2) was resolved on 10% SDS-PAGE and stained with Coomassie Brilliant Blue R-250 (left). M, Molecular mass standards in kilodaltons. Similar gels containing less sample (100 ng of protein per lane) were blotted onto nitrocellulose membranes and probed with polyclonal antibodies to PHIP1 (middle) or the preimmune serum (preim. s.; right). Protein bands were visualized on x-ray film after incubation with horseradish peroxidase-conjugated second antibody (goat antibody against rabbit IgG). B, Association of PHIP1 with the membranes. Arabidopsis young seedlings (10 d old) were used to prepare soluble fraction (lane 1; Total S) and membrane pellet (lane 2; Total P). The total membrane pellet was further extracted with 1% Triton X-100 (lanes 3 and 4), 100 mM Na_2CO_3 (pH 11.5; lanes 5 and 6), or 1 M NaI (lanes 7 and 8). Molecular masses of protein markers (in kilodaltons) and the position of PHIP1 are indicated. Note that PHIP1 is present only in the membrane pellet (lane 2), can be partially extracted from the membrane pellet by Triton X-100 (lane 3), and can be removed from the membranes with high-pH solution (lane 5) or chaotropic agent (lane 7).

does not contain a signal peptide sequence for targeting to the secretory pathway. Moreover, it contains three putative nuclear localization sequences within the KRD. Thus, PHIP1 is a putative soluble and possibly nucleus-localized protein.

To verify this, we carried out cellular fractionation, followed by western-blot analysis, in order to determine if PHIP1 is present in the soluble fraction and associated with membranes in plant cells. We first analyzed the specificity of the polyclonal antibodies raised against purified PHIP1 on western blots. The preimmune serum did not react with any visible band (Fig. 3A). The anti-PHIP1 antibody reacted strongly with a 92-kD polypeptide band (GST-PHIP1) but not with the 26-kD GST protein (Fig. 3A). This result indicates that the anti-PHIP1 antibodies recognize specifically PHIP1. Using these antibodies to react with soluble and total membrane fractions on western blots, PHIP1 was found to be tightly associated with the membranes (Fig. 3B, lane 2). No detectable amount of PHIP1 was found in the soluble fraction (Fig. 3B, lane 1). Treatments with an alkaline buffer (Na_2CO_3, pH 11.5) or chaotropic agents (1 M NaI) were able to extract PHIP1 from the membranes (Fig. 3B, lanes 5 and 7), suggesting that PHIP1 is a peripheral membrane protein.

PHIP1 Is Localized at the Cell Plate during Cytokinesis in Plants

Phragmoplastin is associated with the cell plate during cytokinesis in plants (Gu and Verma, 1996, 1997). To test if PHIP1 is colocalized with phragmoplastin at the cell plate during cytokinesis, we performed fluorescence immunocolocalization using antibodies against PHIP1 and phragmoplastin. Purified IgG to phragmoplastin was conjugated with Alexa-488 (a fluorochrome that is excited by 488-nm light and emits green light), whereas IgG to PHIP1 was labeled with Alexa-594, which is excited by 594-nm light and emits red light. Onion (*Allium cepa*) root tip cells were used, since they are large and the cell plate is easy to identify with a fluorescence microscope. Antibodies against either phragmoplastin or PHIP1 reacted with only a protein band of the proper size on western blots of Arabidopsis samples (Fig. 3; Gu and Verma, 1996, 1997). It is likely that both antibodies recognize counterparts of phragmoplastin and PHIP1 in onion samples. Root tip cells were incubated with different fluorochrome-labeled antibodies and visualized using proper sets of optical filters. As shown in Figure 4, C and D, antibodies against PHIP1 (red color) and against phragmoplastin (green color) colocalized at the cell plate in the onion root tip cells. We also determined subcellular localization using transgenic tobacco (*Nicotiana tabacum*) BY-2 cells expressing GFP-PHIP1 (Supplemental Fig. S5E) and showed that the green fluorescence of GFP-PHIP1 was concentrated at the cell plate, while the fluorescence of GFP was excluded from the cell plate in control cells (Supplemental Fig. S5, A–D). These data further confirmed that PHIP1 is associated with the cell plate at cytokinesis in plant cells.

PHIP1 Specifically Binds with the *Ran2* mRNA

Using PHIP1 as bait in the two-hybrid system, we screened an Arabidopsis cDNA library for its interacting partners. We identified several putative PHIP1-interacting clones, among which five were confirmed to interact with PHIP1 using in vitro protein-protein pull-down assays (data not shown). They encode a

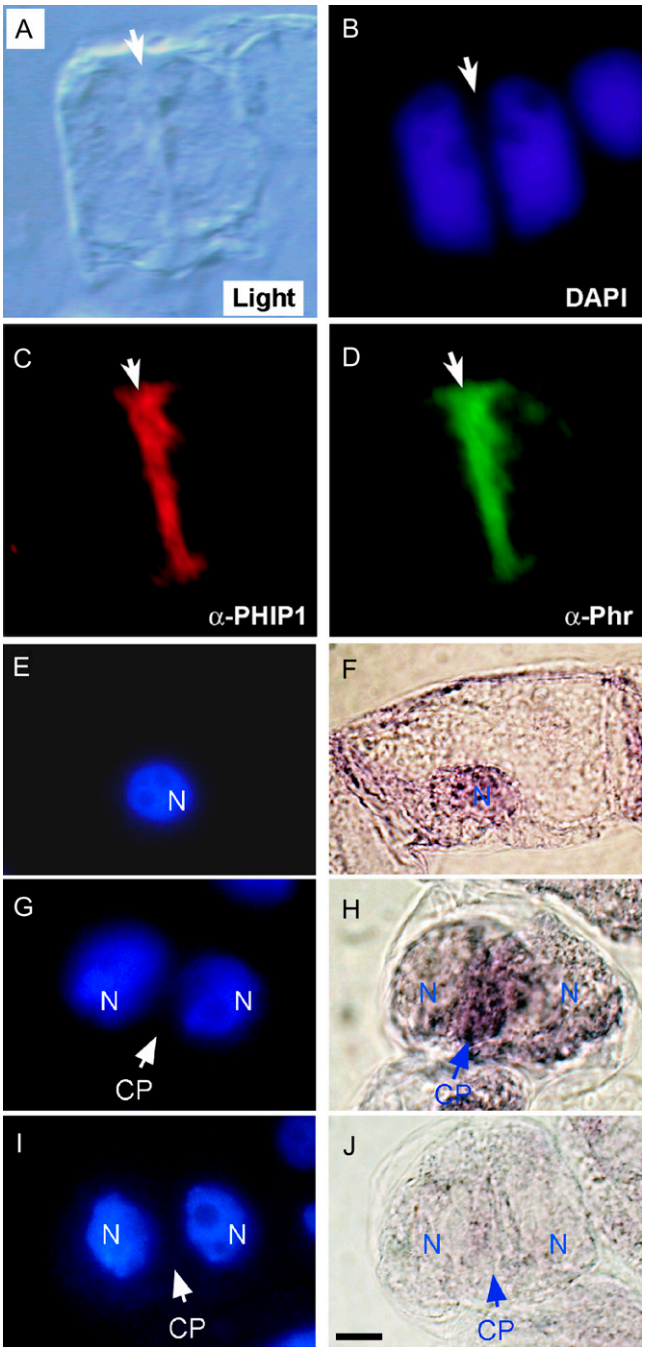

Figure 4. Subcellular localization of PHIP1 and *Ran2* mRNA at cytokinesis. A to D, Direct immunofluorescence localization of PHIP1. Onion root tip cells were fixed in paraformaldehyde and reacted to antibodies against Arabidopsis PHIP1 (α-PHIP1) or soybean phragmoplastin (α-Phr). Antibodies to PHIP1 were conjugated with fluorescent dye Alexa 594 and exhibited red fluorescence, whereas phragmoplastin antibodies conjugated with Alexa 488 emitted green fluorescence. Nuclear DNA was stained with DAPI. The bright-field image (Light) was taken using Normarski optics. Arrows indicate the position of the cell plate. E to J, Whole-mount in situ RNA hybridization. Tobacco BY-2 cells were fixed and reacted with digoxigenin-labeled *Ran2* RNA probes, which were detected by anti-digoxigenin antibody conjugated with alkaline phosphatase (F, H, and J). Nuclear DNA (N) was stained with DAPI and imaged under a UV filter (E, G, and I). A nondividing cell (E and F) and a cytokinetic cell (G and H) with the cell plate (CP) are shown. The Ran2 sense RNA probe was used as a negative control (I and J). Bar = 10 μm.

nitrate reductase (pPHIP-IP-5), a cadmium-induced protein (pPHIP-IP-7), a pentatricopeptide repeat-containing protein (pPHIP-IP-30), a CBL-interacting protein kinase 6 (pPHIP-IP-31), and the small GTP-binding protein Ran2 (pPHIP-IP-33; Ma et al., 2007). Bearing in mind that PHIP1 is a putative RNA-binding protein, we asked if any of these interactions also existed at the protein-mRNA level.

We used GST-tagged PHIP1 to adsorb Arabidopsis total RNA directly, followed by extensive washing and reverse transcription (RT)-PCR using gene-specific primers. RNAs bound to the glutathione beads were extracted by phenol-chloroform solution and reverse transcribed into cDNA. PCR amplification was carried out using five pairs of primers corresponding to the cDNAs of the five PHIP1-interacting partners. As shown in Figure 5A, lane 4, a PCR product band of 0.66 kb was specifically amplified using primer pairs corresponding to the *Ran2* cDNA (pPHIP-IP-33). Four other pairs of primers failed to produce any PCR products under similar RT-PCR conditions, even after using extended cycles (more than 35) of PCR (data not shown). No PCR product was amplified in negative controls in which GST was used instead of GST-PHIP1 (Fig. 5A, lane 1) or when mRNA was used directly to replace the RT product of the PHIP1-bound mRNA as a template for PCR amplification (Fig. 5A, lane 3). These data suggest that PHIP1 interacts with Ran2 protein as well as *Ran2* mRNA.

To confirm the binding of PHIP1 with the *Ran2* mRNA, we carried out a UV cross-linking assay of PHIP1 with ^{32}P-radiolabeled *Ran2* mRNA. Radioactive *Ran2* mRNA was synthesized in vitro using T7 RNA polymerase (Takara) in the presence of [^{32}P]UTP. Purified PHIP1 was incubated with radiolabeled *Ran2* mRNA and irradiated under 360-nm UV light. Unbound mRNA was removed by treatment with RNase A. The cross-linking products of PHIP1 were resolved by SDS-PAGE. As shown in Figure 5B, PHIP1 (lane 2) but not GST (lane 1; negative control) was found to be labeled with the radioactive probe, suggesting that *Ran2* mRNA is bound to PHIP1.

The binding of PHIP1 with the *Ran2* mRNA was further confirmed by RNA electrophoretic mobility-shift assay. For this assay, ^{32}P-labeled *Ran2* mRNA was incubated with purified GST-PHIP1 and resolved on a 0.7% agarose gel. The mobility of *Ran2* mRNA was clearly shifted by treatment with PHIP1 (Fig. 5C, lane 3) but not GST (Fig. 5C, lane 2). These results further confirm that PHIP1 is an RNA-binding protein and binds specifically to *Ran2* mRNA. We further reasoned that Ran2 mRNA might be distributed toward the cell plate at the subcellular level. We used digoxigenin-labeled antisense *Ran2* mRNA to react with cytokinetic cells and demonstrated that *Ran2* mRNA is indeed highly concentrated in the vicinity of the cell plate (Fig. 4D).

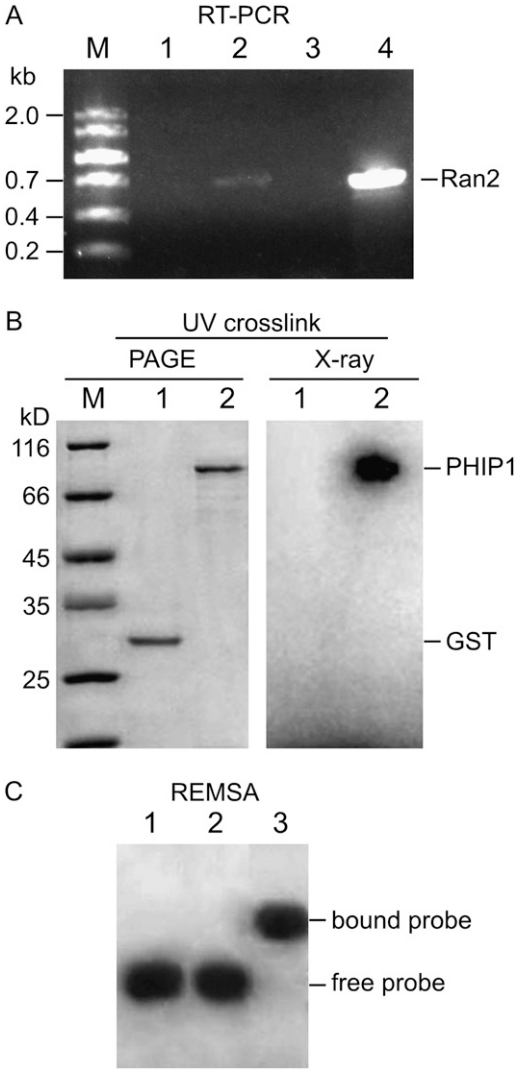

Figure 5. PHIP1 binds *Ran2* mRNA. A, RT-PCR products of *Ran2* mRNA bound to PHIP1. Primers specific to *Ran2* were used for PCR amplification. Lane 1, PCR product using Arabidopsis total RNA without performing RT (negative control). Lane 2, RT-PCR product using Arabidopsis total RNA (positive control). Lane 3, RT-PCR product using RNA bound to the GST beads (negative control). Lane 4, RT-PCR product using RNA extracted from the GST-PHIP1 beads. M, DNA ladder in kilobases. B, UV cross-linking assay of PHIP1 with ^{32}P-labeled *Ran2* mRNA. Left panel, Coomassie Brilliant Blue R-250 staining of SDS-PAGE. Lane 1, Cross-linking product of GST with the [^{32}P]*Ran2* mRNA probe (negative control). M, Molecular mass standards in kilodaltons. Lane 2, Cross-linking product of GST-PHIP1 with [^{32}P]*Ran2* mRNA. Right panel, X-ray autoradiograph of the gel shown at left. C, RNA electrophoretic mobility-shift assay (REMSA) of [^{32}P]*Ran2* mRNA with PHIP1. Lane 1, Free [^{32}P]*Ran2* mRNA probe. Lane 2, [^{32}P]*Ran2* mRNA incubated with GST protein (negative control). Lane 3, [^{32}P]*Ran2* mRNA incubated with GST-PHIP1. Note that the mobility of the [^{32}P]*Ran2* mRNA probe shifted in the presence of PHIP1.

DISCUSSION

PHIP1 Is an RNA-Binding Protein Associated with Cell Plate Formation

Amino acid sequence analysis revealed that PHIP1 does not share overall sequence homology and motif arrangements with any other known genes in GenBank, suggesting that it represents a novel RNA-binding protein. The most homologous genes to Arabidopsis *PHIP1* are two rice sequences (Os05g0114500 in subspecies *japonica* and OsI_017529 in subspecies *indica*). They share approximately 31% identity with *PHIP1* at the amino acid level and contain two RRMs and four CCHC-type ZnFs, as opposed to three ZnFs present in PHIP1. The other major difference is that the rice proteins do not contain a KRD. The function of these rice genes remains unknown.

PHIP1 contains multiple conserved motifs, including two nuclear localization signals in a KRD, two RRMs, and three ZnFs. ZnFs are found in a number of proteins that can bind to DNA, RNA, and DNA-RNA hybrids (Brown, 2005; Hall, 2005; Gamsjaeger et al., 2007). In addition, ZnFs have also been implicated in protein-protein interactions (Mackay and Crossley, 1998; Gamsjaeger et al., 2007). The mammalian transcription factor FRIEND OF GATA1 contains multiple ZnFs, of which the sixth one, a CCHC type, interacts with the N terminus of GATA1 (Tsang et al., 1997). PHIP1 contains three copies of a CCHC-type ZnF with a consensus of Cys-X_2-Cys-X_4-His-X_4-Cys. To assess if these ZnFs are involved in interaction with phragmoplastin, we made a series of deletions that contained two, one, or none of the three ZnFs. The data clearly excluded the involvement of ZnFs in the interaction of PHIP1 with phragmoplastin. The exact role of the ZnFs in PHIP1 remains unknown.

The ZnFs of PHIP1 resemble more closely those of retroviral nucleocapsid proteins (Gamsjaeger et al., 2007). The *gag* gene of retroviruses including HIV encodes the so-called gag precursor that is cleaved into three mature proteins, the matrix protein, the capsid protein, and the nucleocapsid protein. In the mature virus, the matrix protein is associated with the inner side of the lipid envelope, the capsid protein forms the outer shell of the nucleocapsid, and the nucleocapsid proteins are complexed with RNA inside the nucleocapsid. ZnFs of nucleocapsid proteins have been shown to bind to ^{65}Zn on western blots (Bess et al., 1992), but it is not known if these fingers are directly involved in RNA binding.

PHIP1 contains two RRMs that may be involved in the specific binding with the *Ran2* mRNA. These RRMs may function together with the ZnFs and modulate the post-transcriptional regulation of *Ran2* and other genes at cytokinesis. The function of the KRD and the two nuclear localization signals present remain to be determined. It is possible that this protein shuttles between the nucleus and the forming cell plate at cytokinesis and functions in transporting *Ran2* and other mRNAs to the vicinity of the cell plate (Fig. 6). These data are consistent with the observations that Ran2 protein is localized at the cell plate as well as at the nuclear envelope (Ma et al., 2007).

Involvement of Rho-Like Proteins in Cell Plate Formation

The Rho protein family includes Rho, Rac, and Cdc42 (Gu et al., 2004; Brembu et al., 2006). Yeast Cdc42, a Rho

homolog, controls the assembly of polarized complexes at the cell surface that regulate exocytotic secretion and bud formation (Mata and Nurse, 1998). Yeast Rho protein has been found in the cell cortex of a growing bud (Hirata et al., 1998) and has been suggested to control callose synthase activity (Qadota et al., 1996). Plant Rop GTPases (Rho-like proteins) may have functions similar to those of Cdc42 and Rac (Li et al., 1999; Gu et al., 2004; Brembu et al., 2006). We demonstrated that Arabidopsis Rop1 interacts with PHIP1 both in the yeast two-hybrid system and in the in vitro pull-down assay. This is significant because it suggests the possibility that Rho-like proteins may be involved in the control of cell plate formation, probably providing spatial information. Previously, mutations at the conserved GTP-binding motifs of Rop1 were introduced so that the mutated Rop GTPases are locked at either the GTP-bound or GDP-bound conformation (Li et al., 1999). In this study, we examined whether PHIP1 interacts with the GTP-bound or GDP-bound form of Rop GTPase. Our data demonstrated that PHIP1 interacts with the wild-type Rop1 and Rop-GTP mutant but not the GDP-bound form of Rop1 (Fig. 2). This suggests that a GTP-bound, active Rop GTPase may be recruited from the cytoskeleton or membrane compartments to the PHIP1-phragmoplastin complex at the cell plate. Upon hydrolysis of GTP to GDP, the GDP-bound, inactive Rop GTPase may then dissociate from the PHIP1-phragmoplastin complex. This could be one of the mechanisms regulating the activity of phragmoplastin at the forming cell plate and may provide a mechanism for the activation of callose synthase, since Rho is known to control the activity of callose synthase in yeast (Qadota et al., 1996).

Intracellular RNA Distribution and Cell Polarity

Polarized mRNA distribution within a cell was first observed in animal oocytes and has now been found in many cell types, including neurons, fibroblasts, and myoblasts of animal somatic cells (St Johnson, 1995; Mohr, 1999), in embryonic cells of the brown alga *Fucus* (Bouget et al., 1995, 1996), and during seed development (Okita and Choi, 2002; Crofts et al., 2004, 2005). A single mRNA molecule, once targeted to a subcellular location, can be translated multiple times in that location. This can also prevent the expression of the encoded proteins in the wrong region of the cell. The transport of myelin basic protein mRNA from the cell body to the dendrites of dendrocytes in culture occurs along the cytoskeleton and is apparently mediated by a plus end-directed, kinesin-like motor (Ainger et al., 1993). In a developing *Fucus* zygote, *actin* mRNA is first symmetrically distributed and then accumulates at the thallus pole at the time of polar axis fixation. At the end of the first cell division, *actin* mRNA is specifically redistributed from the thallus pole to the forming cell plate. During the second cell division of the embryo, *actin* mRNA continues to accumulate at the cell plate. The third division of the embryo is perpendicular to the first two divisions, and *actin* mRNA does not accumulate at the cell plate (Bouget et al., 1996). Actin has been localized at the cell plate (Endle et al., 1998). Using antibodies against soybean (*Glycine max*) phragmoplastin on a western blot, we were able to detect the presence of a phragmoplastin homolog of the expected molecular mass (about 70 kD) in a crude extract of *Fucus* embryos (L. Ma, B. Xie, Z. Hong, D.P.S. Verma, and Z. Zhang, unpublished data). This result suggests that the basic machinery for cell plate formation may be conserved (Verma and Hong, 2005). In this report, we show that *Ran2* mRNA is also distributed in the vicinity of the cell plate (Fig. 4D). Unlike typical cell plate-specific proteins such as phragmoplastin (Gu and Verma, 1997; Hong et al., 2003), callose synthase 1 (Hong et al., 2001a), and UDP-Glc transferase (Hong et al., 2001b), both *Ran2* mRNA and PHIP1 were not tightly bound to the cell plate. It was recently demonstrated that ribosomes and presumably protein translation exist in the vicinity of the cell plate immediately outside of the cell plate assembly matrix (Seguí-Simarro et al., 2004). Both *Ran2* mRNA and PHIP1 protein may be distributed closely to the cell plate but excluded from the cell plate assembly matrix. Active transport of mRNAs may require the formation of an RNP complex that has been observed in neurons (Spirin, 1994). PHIP1 may be one of the candidates that bind to specific mRNAs and deliver them to the vicinity of the cell plate during cytokinesis in plant cells.

PHIP1 Forms a Complex with Phragmoplastin and Is Targeted to the Cell Plate

Members of the dynamin family share some common properties, including having GTPase activity and

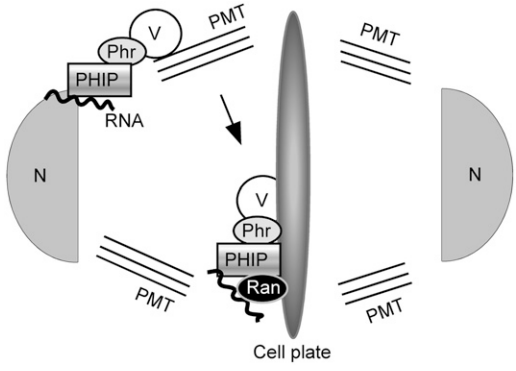

Figure 6. Proposed role of PHIP1 in the polarized RNA transport during cell plate formation. Phragmoplastin (Phr) is associated with the Golgi-derived vesicles that are transported to the cell plate along the phragmoplast microtubules (PMT). PHIP1 contains RRMs and ZnFs and binds specifically with the *Ran2* mRNA (RNA) and possibly with a specific group of other cell plate formation-related mRNAs. The interaction between phragmoplastin and PHIP1 allows the delivery of these mRNAs to the vicinity of the cell plate, where they are translated into proteins (such as Ran2). N, Newly separated daughter nuclei; V, Golgi-derived cell plate vesicles.

the capacity to self-assemble into helical structures (Verma and Hong, 2005). They differ from each other by interacting with different protein partners. Animal dynamin interacts with a number of proteins and plays an important role in clathrin-mediated endocytosis and synaptic vesicle recycling (Schmid et al., 1998). Dynamin is targeted to the coated pits by interacting with amphiphysin and the AP2 complexes, a major constituent of the clathrin coat (David et al., 1996).

Unlike dynamin, phragmoplastin lacks both the pleckstrin homology domain and the Pro-rich domain and performs a very different biological function, regulating the formation of the tubular structures at the cell plate in plants. Several players involved in cell plate formation have been identified (Hong and Verma, 2008). The cloning of PHIP1 has added a distinct member to this group of proteins, which may bind and transport mRNAs such as *Ran2* to the vicinity of the cell plate (Fig. 6). The precise function of PHIP1 in targeting *Ran2* RNA at the cell plate remains to be determined.

MATERIALS AND METHODS

Bacterial and Yeast Strains

Escherichia coli strains DH5α (GIBCO-BRL) and Top10F′ (Invitrogen) were used for plasmid construction and protein expression. DH1 (GIBCO-BRL) was used for plasmid rescue from yeast cells. Yeast (*Saccharomyces cerevisiae*) Y190 (*MATa*, *ura3-52*, *his3-200*, *lys2-801*, *ade2-101*, *trp1-901*, *leu2-3*, *112*, *gal4*Δ, *gal80*Δ, *cyhr2*, *LYS*::*GAL1UAS-HIS3TATA-HIS3*, *URA3*::*GAL1UAS-GAL1TATA-lacZ*) was used as host for two-hybrid experiments.

Screening of a cDNA Library for Interacting Proteins

Full-length phragmoplastin cDNA (pSDL12a; Gu and Verma, 1996) was partially digested with *Bgl*II and *Xho*I, and the fragment (2 kb) was ligated into pAS1-CYH2 vector, generating pAS-Phr. This plasmid was used as bait to screen an Arabidopsis (*Arabidopsis thaliana*) cDNA library constructed in λACT (Kim et al., 1997; Arabidopsis Biological Resource Center, Ohio State University). The cDNA library was converted into plasmid pACT through in vivo excision as described. The pooled plasmids were purified through CsCl ultracentrifugation. Yeast Y190 was first transformed with pAS-Phr by electroporation and selected on synthetic complete (SC) medium without Trp (SC-Trp). Y190 cells containing pAS-Phr were transformed with the Arabidopsis library plasmids by electroporation and selected on SC-Trp-Leu-His medium containing 30 mg L^{-1} 3-amino-1,2,4-triazole (Sigma). Colonies formed in 5 to 7 d were absorbed to 3MM filter discs, permeated by liquid nitrogen, and incubated in Z buffer/X-Gal (120 mM sodium phosphate, pH 7.0, 10 mM KCl, 1 mM $MgCl_2$, 0.2 mM β-mercaptoethanol, and 300 mg L^{-1} X-Gal) for 2 to 10 h. Blue colonies were purified, and plasmids were isolated and propagated in *E. coli* DH1 cells. Purified plasmids were reintroduced into Y190 cells containing pAS-Phr to verify the interaction and to eliminate false positives. Selected cDNAs were sequenced in our automatic DNA sequencing facility.

Deletion Analysis of PHIP1

The plasmid pACT-PHIPZ2, originally obtained from library screening in the yeast two-hybrid system, contained only a partial sequence of the PHIP1 coding region. A full-length cDNA, pPHIP1FL, was obtained by screening an Arabidopsis FL-1 cDNA library constructed in λZapII (provided by Dr. K. Shinozaki, Institute of Physical and Chemical Research). A *Hin*dIII fragment containing the last ZnF motifs was released from the full-length PHIP1 cDNA and subcloned into pACT2, resulting in pACT-PHIPZ1. Plasmid pACT-PHIPKR contains a PCR fragment amplified using T3 and P34RBD-*Xho* primers (5′-CACTCGAGTTGACCTTACTGCTGCTAA-3′). The insert in pACT-PHIPZ was amplified using the T7 and P34Zn-BH primers (5′-AGGGATCCCAGCTACTGATCATACACC-3′). A pair of primers (P34C5, 5′-GAGGATCCAAGAGATTGAAGTTAATACAGAC-3′; and P34B3, 5′-CGCTCGAGTCATCAGCCTTGTTTTTGCAC-3′) was used to amplify a fragment for constructing pACT-PHIPRZ. Two PCR fragments amplified by P34A5 (5′-AGGGATCCAGATGGTGCTGTCGAACAAG-3′) and P34A3 (5′-TCTGTCGAATTCGTTAGGAACAACCCCATCTTC-3′) and by P34B5 (5′-AACGAATTCGACAGACCAGCTACTGATCATACA-3′) and P34B3, respectively, were ligated at the *Eco*RI site and used to generate pACT-PHIPKZ. pACT-PHIPR contains an insert amplified by P34C5 and P34RBD-*Xho* primers.

Expression and Purification of GST Fusion Proteins

A plasmid (pGST-Phr) expressing a GST-phragmoplastin fusion protein was constructed by inserting a *Sma*I-*Xho*I fragment from pACT-Phr into the same sites of pGEX-KG (Frangioni and Neel, 1993). GST-Rop1 fusion protein was expressed from pGEX-R1A (Li et al., 1999; Wu et al., 2000), which was made by cloning a *Nco*I-*Sst*I fragment containing the coding region of Arabidopsis Rop1 cDNA into the same sites of pGEX-KG and transformed into *E. coli* JM109. Expression of GST fusion proteins was induced by 1 mM isopropylthio-β-galactoside for 4 h. Cells were washed and resuspended in STE buffer (10 mM Tris-Cl, pH 8.0, 150 mM NaCl, and 1 mM EDTA). After incubation with 100 μg mL^{-1} lysozyme for 5 min, cells were lysed in the presence of 0.5% sarkosyl followed by sonication (Frangioni and Neel, 1993). The supernatant was diluted with Triton X-100 to a final concentration of 1% and incubated with glutathione-agarose beads (Sigma) followed by extensive washing with STE buffer.

Detection of Protein-Protein Interaction by in Vitro Pull-Down Assay

For in vitro labeling of PHIP1, a *Sal*I fragment encoding a partial PHIP1 peptide lacking the first 96 amino acid residues was subcloned into the same site of pAGA3 (Sanford et al., 1991) that contains a hemoglobin 5′-leader sequence under the T7 promoter. The resulting plasmid, pAGA-PHIP1, was used for quick-coupled transcription/translation in the TNT-T7 system (Promega) in the presence of [^{35}S]Met (Amersham). Radiolabeled PHIP1 product (10 μL) was diluted in 260 μL of interaction buffer (20 mM Tris-Cl, pH 8.0, 100 mM KCl, 2 mM $MgCl_2$, 0.5% lubral, and 0.5% bovine serum albumin) and incubated with 10 μL of purified GST fusion proteins bound to glutathione-agarose beads for 1 h. The beads were washed five times with the interaction buffer without bovine serum albumin, and the bound proteins were eluted directly in SDS-PAGE sample buffer. After electrophoresis, the gel was stained with Coomassie Brilliant Blue R-250, dried, and autoradiographed.

GST Fusion Protein Purification and Preparation of Antibodies

For the purification of PHIP1 protein from *E. coli*, a *Bam*HI-*Xho*I fragment encoding the partial PHIP1 peptide (lacking the first 53 amino acid residues) was excised from pPI34 obtained from the original screening of the Arabidopsis cDNA library in the yeast two-hybrid system. The fragment was inserted into the same sites of pGEX-KG, generating pGST-PHIP1 that expressed a GST-PHIP1 fusion protein. The plasmids were transformed to *E. coli* strain JM109, and expression of the fusion protein was induced by isopropylthio-β-galactoside. GST-PHIP1 was purified using glutathione-agarose beads (Sigma). GST tag was cleaved by incubating the bead-bound GST-PHIP1 with thrombin (2 units mL^{-1}; Sigma) in the thrombin buffer (50 mM Tris-Cl, pH 8.0, 150 mM NaCl, 2.5 mM $CaCl_2$, and 0.1% β-mercaptoethanol). The cleaved products were resolved on 10% PAGE. PHIP1 bands from 10 gels containing about 1 mg of PHIP1 protein was excised, eluted with 0.85% NaCl, lyophilized, and used to raise antibodies in two rabbits. For purification of antibodies against PHIP1, purified GST-PHIP1 fusion protein was resolved on PAGE and transferred to nitrocellulose. The membrane containing the PHIP1 band was excised, blocked with 5% nonfat milk in phosphate-buffered saline (PBS), and used to react with PHIP1 antibody in a serum:PBS (1:2) solution. Antibodies bound to the membrane slices were eluted by 100 mM Gly (pH 2.5), and the eluted antibodies were immediately neutralized by 1 M Tris (pH 8.0) solution.

Preparation of Plant Samples and Western-Blot Analysis

Arabidopsis young seedlings (10 d old) were frozen in liquid nitrogen and ground into powder with a mortar and pestle. The powder was resuspended in extraction buffer (50 mM Tris-Cl, pH 7.5, 100 mM NaCl, 2 mM β-mercaptoethanol, and 1 mM phenylmethylsulfonyl fluoride). The homogenate was spun at 10,000*g* for 15 min, and the supernatant was further separated into supernatant (100S) and membrane (100P) fractions by ultracentrifugation at 100,000*g* for 90 min. The total membrane pellet was extracted with 1% Triton X-100 in extraction buffer, 100 mM Na_2CO_3 (pH approximately 11.5), or 1 M NaI in extraction buffer, followed by centrifugation at 100,000*g* for 30 min. Fractions were adjusted to 1× SDS loading buffer and resolved on SDS-PAGE. Proteins were transferred to a polyvinylidene difluoride membrane (Amersham) and probed with purified PHIP1 antibody. Horseradish peroxidase-labeled goat antibody against rabbit IgG was used as a secondary antibody. The protein bands were visualized on Kodak BioMax MS film using Super-Signal West Pico Chemiluminescent Substrate (Pierce). Purified GST and GST-PHIP1 fusion protein were used as negative and positive controls, respectively. In another negative control, the preimmune serum was used to replace the first antibody.

Expression of GFP-PHIP1 in Tobacco BY-2 Cells

The PHIP1 cDNA was cloned at the *Eco*RI site of pMON-GFP (Hong et al., 2001a). The coding region of PHIP1 was fused in-frame with the GFP cDNA downstream of the cauliflower mosaic virus 35S promoter (Fig. 6I). The whole cassette was released by *Not*I and cloned into the same site of pMON18342 (Hong et al., 2001a), generating pMBin-GFP-PHIP1. Plasmid pMON30066 expressing GFP served as a control. Tobacco (*Nicotiana tabacum*) BY-2 cells were transformed via *Agrobacterium tumefaciens*-mediated procedures (Gu and Verma, 1997).

Immunofluorescence Microscopy

Affinity purified IgGs against PHIP1 and phragmoplastin were conjugated with the fluorescent dyes Alexa 594 and Alexa 488 (Molecular Probes), respectively, following the manufacturer's instructions. Onion (*Allium cepa*) root tips were fixed in 4% paraformaldehyde and 15% Suc in PHEM buffer (60 mM PIPES, 25 mM HEPES, pH 6.9, 10 mM EGTA, and 2 mM $MgCl_2$) at room temperature for 3 h. The samples were washed with washing buffer (10 mM MES, pH 5.7, 30 mM $CaCl_2$, 5 mM β-mercaptoethanol, 400 mM mannitol, and 0.1% bovine serum albumin) three times for 10 min each. The tissues were digested with freshly prepared digestion buffer (2% cellulase, 1% Macerozyme R-10, 0.5% pectinase, and 0.5% Driselase in washing buffer) for 30 min, followed by rinsing with PHEM buffer two times for 5 min each. Root tips were squeezed between two poly-Lys-coated glass slides. Cells were permeated with 0.2% Triton X-100 in PHEM for 5 min and extracted by −20°C methanol:acetone (1:1) for 10 min. The cells were blocked with 1% nonfat milk in PHEM for 1 h and reacted with Alexa dye-labeled antibody for 1 h. The slides were washed with PBS containing 0.5% Tween 20 and 1 μg mL^{-1} 4′,6-diamidino-2-phenylindole (DAPI). Fluorescence microscopy was carried out in a Zeiss microscope with appropriate filters.

Affinity Adsorption Assay

GST-PHIP1 bound to the glutathione beads was incubated with the total RNA from 6- to 8-d-old Arabidopsis seedlings for 1 h on ice with slight shaking. The beads were washed three times with binding buffer (50 mM Tris-HCl, 1 mM phenylmethylsulfonyl fluoride, 5 units of RNasin, 2 mM β-mercaptoethanol, and 0.01 mM EDTA). RNAs bound to the beads were extracted by phenol:chloroform:amyl alcohol (49:49:2) two times with vigorous shaking. The eluted RNAs were precipitated with 95% ethanol at −20°C for 30 min. The RNA pellet was washed with 75% ethanol, briefly dried in air, and dissolved with diethyl pyrocarbonate-treated water. The eluted RNAs were reverse transcribed into cDNA using the PCR Kit (Amv) version 3.0 (Takara). The identity of the eluted RNAs was profiled by RT-PCR amplification analysis using five pairs of primers corresponding to five Arabidopsis cDNAs that were previously identified as protein-protein interaction partners of PHIP1 in a yeast two-hybrid screen (L. Ma, B. Xie, Z. Hong, D.P.S. Verma, and Z. Zhang, unpublished data). The following five pairs of primers were used in this experiment: 5′-AGTCGACATGACTTCTTTCTCTCTCAC-3′ and 5′-GGAATTCATCTTCATTCTCTTCTCTTTCTC-3′ for PHIP-IP-5 (encoding a nitrate reductase); 5′-CGGTCGACATGGTCTTGATGATCATTA-3′ and 5′-CGGGAATTCTTACATAGCTGATGATTTA-3′ for PHIP-IP-7 (encoding a cadmium-induced protein); 5′-CCGTCGACATGTACATAGAAATTGCTTC-3′ and 5′-CGGAATTCACCAGGAAATGGCTTTAAG-3′ for PHIP-IP-30 (a pentatricopeptide repeat-containing protein); 5′-AAGTCGACATGGTCGGAGCAAAACCGG-3′ and 5′-CGGAATTCAGCAGGTGTAGAGGTCCAG-3′ for PHIP-IP-31 (a CBL-interacting protein kinase); and 5′-CGTCGACATGGCTCTACCTAACCAAC-3′ and 5′-CGGAATTCTTACTCAAATGCGTCATCA-3′ for PHIP-IP-33 (encoding the small GTPase Ran2; Ma et al., 2007). PCR amplification conditions were set differently for each gene on the basis of the annealing temperatures of the primers and the lengths of the expected PCR products. A series of PCR cycles from 25 to 35 were performed for each gene. Only the *Ran2* mRNA (PHIP-IP-33) was detected under these RT-PCR conditions, while RT-PCR for the other four mRNAs failed to amplify any PCR products. The PCR conditions used for successful detection of the *Ran2* mRNA (PHIP-IP-33) were 28 cycles at 94°C for 30 s, 63°C for 45 s, and 72°C for 45 s. GST bound to beads was treated as described above and served as a negative control.

Radiolabeling of RNA Transcripts

Radioactive mRNA probe was prepared essentially as described elsewhere (Vaquero et al., 1998) with some modifications. The *Ran2* cDNA (0.66 kb), cloned in pTYB2 vector, was transcribed in vitro in the presence of [α-^{32}P]rUTP using T7 RNA polymerase. The reaction mixture (30 μL) contained 1× T7 RNA polymerase buffer, 5 mM dithiothreitol, 0.5 mM rATP, rCTP, and rGTP each, 12 μM rUTP, 1.7 μCi μL^{-1} [α-^{32}P]rUTP, 9.2 units μL^{-1} RNasin, approximately 2.3 to 11.5 units μL^{-1} T7 RNA polymerase, and 750 ng of linearized pTYB2-Ran2. After incubation at 37°C for 30 min, the template was removed by treatment with 3 μL of RNase-free DNase I (5 units μL^{-1}). The ^{32}P-labeled *Ran2* mRNA probe was purified according to the manufacturer's instructions (Takara).

UV Cross-Linking Assay

A modified protocol as described previously by Vaquero et al. (1998), Sladic et al. (2004), and Sully et al. (2004) was adopted for the UV cross-linking assay. Purified GST-PHIP1 protein was incubated with 15 ng of [^{32}P]*Ran2* mRNA in a reaction mix of 48 μL containing 10 mM Tris-HCl, pH 8.0, 50 mM NaCl, 1 mM EDTA, 1 mM phenylmethylsulfonyl fluoride, 1 mM benzamide, and 0.05 units μL^{-1} RNasin for 30 min at 4°C with slight shaking. The reaction mix was irradiated under 360-nm UV light over a distance of approximately 3 to 5 cm on ice for 90 min. The UV-irradiated sample was treated with 1.5 μg of RNase A for 15 min at 37°C to remove unbound RNA and boiled for 5 min in 3× SDS loading buffer (6% SDS, 87.5 mM Tris, pH 6.8, 30% glycerol, and 0.03% bromphenol blue). Proteins were resolved on 10% SDS-PAGE. The PAGE gel was stained with Coomassie Brilliant Blue G-250, dried, and autoradiographed by exposure to x-ray film at −80°C for 20 to 48 h. GST protein treated with the same procedures served as a negative control.

RNA Electrophoretic Mobility Shift Assays

Purified GST-PHIP1 was incubated with 10 ng of [^{32}P]*Ran2* mRNA in a total volume of 32 μL of reaction buffer for 30 min at 4°C with slight shaking. The RNA products were separated on a 0.7% agarose gel. After electrophoresis, the gel was dried and autoradiographed at −80°C for 8 to 24 h. GST protein treated with the same procedures served as a negative control.

Whole-Mount mRNA Hybridization

Arabidopsis *Ran2* cDNA was amplified from total mRNA by RT-PCR using primers Ran2-F1 (5′-ACCTCGAGATGGCTCTACCTAACCAAC-3′) and Ran2-R1 (5′-ACCTCGAGCTCAAATGCGTCATCATC-3′). The cDNA was cloned in pCR2.1 (Invitrogen) and used as a template for the synthesis of antisense RNA (negative control) and sense RNA probes using a digoxigenin RNA labeling kit (Roche). Tobacco BY-2 cells were fixed in the fixative solution (4% [w/v] paraformaldehyde, 15% [v/v] dimethyl sulfoxide, 0.1% [v/v] Tween 20, and 3% [w/v] Suc in PBS) for 1 h. After washing with PBS solution containing 0.1% (v/v) Tween 20, the cells were hybridized with the labeled

RNA probes at 55°C overnight, followed by hybridization with anti-digoxigenin antibody (1:2,000) conjugated with alkaline phosphatase (Hejatko et al., 2006). DAPI (1 μg mL^{-1}) was supplemented in the second antibody solution, and the fluorescence was observed under a UV filter.

Sequence data from this article can be found in the GenBank/EMBL data libraries under accession number AF196776.

Supplemental Data

The following materials are available in the online version of this article.

Supplemental Figure S1. Interaction of phragmoplastin with PHIP1 in the yeast two-hybrid system.

Supplemental Figure S2. Multiple functional motifs of PHIP1.

Supplemental Figure S3. Domains of PHIP1 responsible for its interaction with phragmoplastin and Rop1.

Supplemental Figure S4. Detection of interaction between PHIP1 and Rop1 by in vitro pull-down assay.

Supplemental Figure S5. Subcellular localization of GFP-PHIP1.

ACKNOWLEDGMENTS

We thank Dr. Zhenbiao Yang for providing Arabidopsis Rop1 plasmids, the Arabidopsis Biological Resource Center for cDNA library CD4-22, and Dr. K. Shinozaki for the Arabidopsis FL-1 cDNA library. We also thank Prof. Yucai Liao for advice on RNA-binding assays.

Received April 4, 2008; accepted July 7, 2008; published July 11, 2008.

LITERATURE CITED

Ainger K, Avossa D, Morgan F, Hill SJ, Barry C, Barbarese E, Carson JH (1993) Transport and localization of exogenous myelin basic protein mRNA microinjected into oligodendrocytes. J Cell Biol **123:** 431–441

Berg JM (1986) Potential metal-binding domains in nucleic acid binding proteins. Science **232:** 485–487

Bess JW Jr, Powell PJ, Issaq HJ, Schumack LJ, Grimes MK, Henderson LE, Arthur LO (1992) Tightly bound zinc in human immunodeficiency virus type 1, human T-cell leukemia virus type I, and other retroviruses. J Virol **66:** 840–847

Bouget FY, Gerttula S, Quatrano RS (1995) Spatial redistribution of poly(A)$^+$ RNA during polarization of the *Fucus* zygote is dependent upon microfilaments. Dev Biol **171:** 258–261

Bouget FY, Gerttula S, Shaw S, Quatrano RS (1996) Localization of actin mRNA during the establishment of cell polarity and early cell divisions in *Fucus* embryos. Plant Cell **8:** 189–201

Brembu T, Winge P, Bones AM, Yang Z (2006) A RHOse by any other name: a comparative analysis of animal and plant Rho GTPases. Cell Res **16:** 435–445

Brown RS (2005) Zinc finger proteins: getting a grip on RNA. Curr Opin Struct Biol **15:** 94–98

Crofts AJ, Washida H, Okita TW, Ogawa M, Kumamaru T, Satoh H (2004) Targeting of proteins to endoplasmic reticulum-derived compartments in plants: the importance of RNA localization. Plant Physiol **136:** 3414–3419

Crofts AJ, Washida H, Okita TW, Satoh M, Ogawa M, Kumamaru T, Satoh H (2005) The role of mRNA and protein sorting in seed storage protein synthesis, transport, and deposition. Biochem Cell Biol **83:** 728–737

David C, McPherson PS, Mundigl O, de Camilli P (1996) A role of amphiphysin in synaptic vesicle endocytosis suggested by its binding to dynamin in nerve terminals. Proc Natl Acad Sci USA **93:** 331–335

Dreyfuss G, Philipson L, Mattaj IW (1988) Ribonucleoprotein particles in cellular processes. J Cell Biol **106:** 1419–1425

Endle MC, Stoppin V, Lambert AM, Schmit AC (1998) The growing cell plate of higher plants is a site of both actin assembly and vinculin-like antigen recruitment. Eur J Cell Biol **77:** 10–18

Erard M, Barker DG, Amalric F, Jeang KT, Gatignol A (1998) An Arg/Lys-rich core peptide mimics TRBP binding to the HIV-1 TAR RNA upper-stem/loop. J Mol Biol **279:** 1085–1099

Frangioni JV, Neel BG (1993) Solubilization and purification of enzymatically active glutathione S-transferase (pGEX) fusion proteins. Anal Biochem **210:** 179–187

Gamsjaeger R, Liew CK, Loughlin FE, Crossley M, Mackay JP (2007) Sticky fingers: zinc-fingers as protein-recognition motifs. Trends Biochem Sci **32:** 63–70

Gu X, Verma DPS (1996) Phragmoplastin, a dynamin-like protein associated with cell plate formation in plants. EMBO J **15:** 695–704

Gu X, Verma DPS (1997) Dynamics of phragmoplastin in living cells during cell plate formation and uncoupling of cell elongation from the plane of cell division. Plant Cell **9:** 157–169

Gu Y, Wang Z, Yang Z (2004) ROP/RAC GTPase: an old new master regulator for plant signaling. Curr Opin Plant Biol **7:** 527–536

Hall TM (2005) Multiple modes of RNA recognition by zinc finger proteins. Curr Opin Struct Biol **15:** 367–373

Hejatko J, Blilou I, Brewer PB, Friml J, Scheres B, Benkova E (2006) In situ hybridization technique for mRNA detection in whole mount Arabidopsis samples. Nat Protocols **1:** 1939–1946

Hirata D, Nakano K, Fukui M, Takenaka H, Miyakawa T, Mabuchi I (1998) Genes that cause aberrant cell morphology by overexpression in fission yeast: a role of a small GTP-binding protein Rho2 in cell morphogenesis. J Cell Sci **111:** 149–159

Hong Z, Delauney A, Verma DPS (2001a) A cell plate-specific callose synthase and its interaction with phragmoplastin and UDP-glucose transferase. Plant Cell **13:** 755–768

Hong Z, Geisler-Lee J, Zhang Z, Verma DPS (2003) Phragmoplastin dynamics: multiple forms, microtubule association and their roles in cell plate formation in plants. Plant Mol Biol **53:** 297–312

Hong Z, Verma DPS (2008) Molecular analysis of the cell plate forming machinery. *In* DPS Verma, Z Hong, eds, Cell Division Control in Plants. Springer, Berlin, pp 303–320

Hong Z, Zhang ZM, Olson JM, Verma DPS (2001b) A novel UDP-glucose transferase is part of the callose synthase complex and interacts with phragmoplastin at the forming cell plate. Plant Cell **13:** 769–779

Huang J, Kleinberg ME (1999) Activation of the phagocyte NADPH oxidase protein p47(phox): Phosphorylation controls SH3 domain-dependent binding to p22 (phox). J Biol Chem **274:** 19731–19737

Kieber JJ, Rothenberg M, Roman G, Feldmann KA, Ecker JR (1993) CTR1, a negative regulator of the ethylene response pathway in Arabidopsis, encodes a member of the raf family of protein kinases. Cell **72:** 427–441

Kim J, Harter K, Theologis A (1997) Protein-protein interactions among the Aux/IAA proteins. Proc Natl Acad Sci USA **94:** 11786–11791

Li H, Lin Y, Heath RM, Zhu MX, Yang Z (1999) Control of pollen tube tip growth by a Rop GTPase-dependent pathway that leads to tip-localized calcium influx. Plant Cell **11:** 1731–1742

Lutcke HA, Chow KC, Mickel FS, Moss KA, Kern HF, Scheele GA (1987) Selection of AUG initiation codons differs in plants and animals. EMBO J **6:** 43–48

Ma L, Hong Z, Zhang Z (2007) Perinuclear and nuclear envelope localizations of Arabidopsis Ran proteins. Plant Cell Rep **26:** 1373–1382

Mackay JP, Crossley M (1998) Zinc fingers are sticking together. Trends Biochem Sci **23:** 1–4

Maris C, Dominguez C, Allain FH (2005) The RNA recognition motif, a plastic RNA-binding platform to regulate post-transcriptional gene expression. FEBS J **272:** 2118–2131

Mata J, Nurse P (1998) Discovering the poles in yeast. Trends Cell Biol **8:** 163–167

Matthews JM, Sunde M (2002) Zinc fingers: folds for many occasions. IUBMB Life **54:** 351–355

Mohr E (1999) Subcellular RNA compartmentalization. Prog Neurobiol **57:** 507–525

Okita TW, Choi SB (2002) mRNA localization in plants: targeting to the cell's cortical region and beyond. Curr Opin Plant Biol **5:** 553–559

Qadota H, Python CP, Inoue SB, Arisawa M, Anraku Y, Zheng Y, Watanabe T, Levin DE, Ohya Y (1996) Identification of yeast Rho1p GTPase as a regulatory subunit of 1,3-beta-glucan synthase. Science **272:** 279–281

Samuels AL, Giddings TH, Staehelin LA (1995) Cytokinesis in tobacco BY-2 and root tip cells: a new model of cell plate formation in higher plants. J Cell Biol **130:** 1345–1357

Sanford J, Codina J, Birnbaumer L (1991) Gamma-subunits of G proteins,

but not their alpha- or beta-subunits, are polyisoprenylated: studies on post-translational modifications using in vitro translation with rabbit reticulocyte lysates. J Biol Chem **266:** 9570–9579

Schmid SL, McNiven MA, De Camilli P (1998) Dynamin and its partners: a progress report. Curr Opin Cell Biol **10:** 504–512

Schwieger C, Blume A (2007) Interaction of poly(L-lysines) with negatively charged membranes: an FT-IR and DSC study. Eur Biophys J **36:** 437–450

Seguí-Simarro JM, Austin JR II, White EA, Staehelin LA (2004) Electron tomographic analysis of somatic cell plate formation in meristematic cells of *Arabidopsis* preserved by high-pressure freezing. Plant Cell **16:** 836–856

Seki M, Carninci P, Nishiyama Y, Hayashizaki Y, Shinozaki K (1998) High efficiency cloning of Arabidopsis full-length cDNA by biotinylated CAP trapper. Plant J **15:** 707–720

Sladic RT, Lagnado CA, Bagley CJ, Goodall GJ (2004) Human PABP binds AU-rich RNA via RNA-binding domains 3 and 4. Eur J Biochem **271:** 450–457

Spirin AS (1994) Storage of messenger RNA in eukaryotes: envelopment with protein, translational barrier at 5′ side, or conformational masking by 3′ side? Mol Reprod Dev **38:** 107–117

Staehelin LA, Hepler PK (1996) Cytokinesis in higher plants. Cell **84:** 821–824

St Johnson D (1995) The intracellular localization of messenger RNAs. Cell **81:** 167–170

Sully G, Dean JL, Wait R, Rawlinson L, Santalucia T, Saklatvala J, Clark AR (2004) Structural and functional dissection of a conserved destabilizing element of cyclo-oxygenase-2 mRNA: evidence against the involvement of AUF-1 [AU-rich element/poly (U)-binding/degradation factor-1], AUF-2, tristetraprolin, HuR (Hu antigen R) or FBP1 (far-upstream-sequence-element-binding protein 1). Biochem J **377:** 629–639

Tsang AP, Fujiwara Y, Hom DB, Orkin SH (1997) Failure of megakaryopoiesis and arrested erythropoiesis in mice lacking the GATA-1 transcriptional cofactor FOG. Genes Dev **12:** 1176–1188

Van de Bor V, Davis I (2004) mRNA localisation gets more complex. Curr Opin Cell Biol **16:** 300–307

Vaquero C, Liao YC, Fischer R (1998) Nonradioactive UV cross-linking assay for the study of protein-RNA binding. Biotechniques **24:** 68–72

Verma DPS (2001) Cytokinesis and building of the cell plate in plants. Annu Rev Plant Physiol Plant Mol Biol **52:** 751–784

Verma DPS, Hong Z (2005) The ins and outs in membrane dynamics: tubulation and vesiculation. Trends Plant Sci **10:** 159–165

Wu G, Li H, Yang Z (2000) Arabidopsis RopGAPs are a novel family of Rho GTPase-activating proteins that require the Cdc42/Rac-interactive binding motif for Rop-specific GTPase stimulation. Plant Physiol **124:** 1625–1636

Zhang Z, Hong Z, Verma DPS (2000) Phragmoplastin polymerizes into spiral coiled structures *via* intermolecular interaction of two self-assembly domains. J Biol Chem **275:** 8779–8784